# Supercomputer Simulation of Radio-frequency Hepatic Tumor Ablation

N. Kosturski and S. Margenov

*Acad. G. Bonchev str., bl. 25A, 1113 Sofia, Bulgaria*

**Abstract.** We simulate the thermal and electrical processes, involved in the radio-frequency (RF) ablation procedure. The mathematical model consists of two parts – electrical and thermal. The energy from the applied AC voltage is determined first, by solving the Laplace equation to find the potential distribution. After that, the electric field intensity and the current density are directly calculated. Finally, the heat transfer equation is solved to determine the temperature distribution. Heat loss due to blood perfusion is also accounted for.

The representation of the computational domain is based on a voxel mesh. Both partial differential equations are discretized in space via linear conforming FEM. After the space discretization, the backward Euler scheme is used for the time stepping.

Large-scale linear systems arise from the FEM discretization. Moreover, they are ill-conditioned, due to the strong coefficient jumps and the complex geometry of the problem. Therefore, efficient parallel solution methods are required.

The developed parallel solver is based on the preconditioned conjugate gradient (PCG) method. As a preconditioner, we use BoomerAMG – a parallel algebraic multigrid implementation from the package Hypre, developed in LLNL, Livermore.

Parallel numerical tests, performed on the IBM Blue Gene/P massively parallel computer are presented.

**Keywords:** Radio-frequency ablation, Bio-heat equation, FEM, PCG.
**PACS:** 02.60.Cb, 02.60.Dc, 02.60.Lj, 02.70.Dh

## INTRODUCTION

The liver is a common location of tumors. However, not all patients are candidates for surgical resection, due to various criteria. Alternative techniques for treating this disease are needed. RF ablation is a low invasive technique for the treatment of hepatic tumors, utilizing AC current to destroy the tumor cells by heating ([5, 6]). The destruction of the cells occurs at temperatures of 45°C–50°C. The procedure is relatively safe, as it does not require open surgery.

The considered RF probe is illustrated on Figure 1. It consists of a stainless steel trocar with four nickel-titanium retractable electrodes. Polyurethane is used to insulate the trocar. The RF ablation procedure starts by placing the straight RF probe inside the tumor. The surgeon performs this under computer tomography (CT) or ultrasound guidance. Once the probe is in place, the electrodes are deployed and RF current is initiated. Both the surfaces areas of the uninsulated part of the trocar and the electrodes conduct RF current.

Mathematical models improve our understanding of the physical processes during the RF ablation procedure, which can aid in decreasing the posttreatement recurrence rate of this type of treatment. Computer simulation is a powerful tool for predicting the

CP1301, *Applications of Mathematics in Technical and Natural Sciences (AMiTaNS '10)*
edited by M. D. Todorov and C. I. Christov

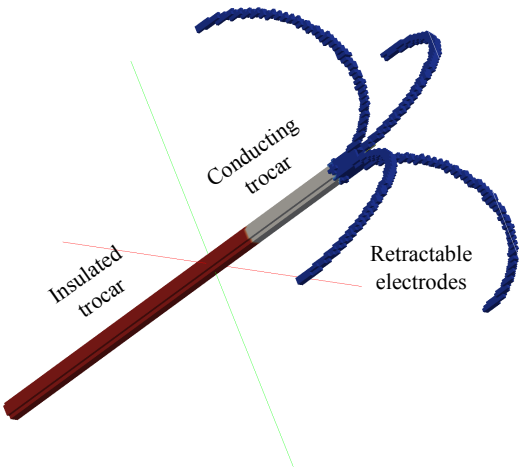


**FIGURE 1.** The structure of a fully deployed RF probe

outcome of the RF ablation procedure in various settings. The aim is to destroy all the tumor cells, without destroying too many healthy cells. Overheating the tissue around the ablation probe must also be avoided. The duration of the procedure should be as short as possible, not exceeding 8 minutes. Computer simulation can be used for designing new ablation probes, as well as for determining the optimal settings (power, duration, probe placement, etc.) in individual cases.

The human liver has a very complex structure, composed of materials with unique thermal and electrical properties. There are three types of blood vessels with different sizes and flow velocities. Large blood vessels affect the RF ablation procedure in two ways. First, when the blood vessels are located close to the ablation electrodes, they affect the electrical field, because of the higher electrical conductivity of the blood. Second, the blood, flowing through the large blood vessels acts like a heat sink, decreasing the temperature around them.

Here, we consider a simplified test problem, where the liver consists of homogeneous hepatic tissue and blood vessels. However, our implementation is capable of utilizing patient specific data for the liver and tumor geometry to realistically simulate the process.

## THE MATHEMATICAL MODEL

The RF ablation procedure destroys the unwanted tissue by heating, arising when the energy dissipated by the electric current flowing through a conductor is converted to heat. The bio-heat time-dependent partial differential equation [5, 6]

$$\rho c \frac{\partial T}{\partial t} = \nabla \cdot k \nabla T + J \cdot E - h_{bl}(T - T_{bl}) \tag{1}$$

is used to model the heating process during the RF ablation. The term $J \cdot E$ in (1) represents the thermal energy arising from the current flow and the term $h_{bl}(T - T_{bl})$ accounts for the heat loss due to blood perfusion.

The following initial and boundary conditions are applied

$$\begin{aligned} T &= 37^{\circ}\text{C when } t = 0 \text{ at } \Omega, \\ T &= 37^{\circ}\text{C when } t \geq 0 \text{ at } \partial\Omega. \end{aligned} \tag{2}$$

The following notations are used in (1) and (2):

- $\Omega$ – the entire domain of the model;
- $\partial\Omega$ – the boundary of the domain;
- $\rho$ – density (kg/m$^3$);
- $c$ – specific heat (J/kg K);
- $k$ – thermal conductivity (W/m K);
- $J$ – current density (A/m);
- $E$ – electric field intensity (V/m);
- $T_{bl}$ – blood temperature (37°C);
- $w_{bl}$ – blood perfusion (1/s);
- $h_{bl} = \rho_{bl} c_{bl} w_{bl}$ – convective heat transfer coefficient accounting for the blood perfusion in the model.

The bio-heat problem is solved in two steps. The first step is finding the potential distribution $V$ of the current flow. With the considered RF probe design, the current is flowing from the conducting electrodes to a dispersive electrode on the patient's body. The electrical flow is modelled by the Laplace equation

$$\nabla \cdot \sigma \nabla V = 0, \tag{3}$$

with boundary conditions

$$\begin{aligned} V &= 0 \text{ at } \partial\Omega, \\ V &= V_0 \text{ at } \partial\Omega_{el}. \end{aligned}$$

The following notations are used in the above equations:

- $V$ – potential distribution in $\Omega$;
- $\sigma$ – electric conductivity (S/m);
- $V_0$ – applied RF voltage;
- $\partial\Omega_{el}$ – surface of the conducting part of the RF probe.

After determining the potential distribution, the electric field intensity can be computed from

$$E = -\nabla V,$$

and the current density from

$$J = \sigma E.$$

The second step is to solve the heat transfer equation (1) using the heat source $J \cdot E$ obtained in the first step.

## NUMERICAL TREATMENT

For the numerical solution of both of the above discussed steps of the simulation the Finite Element Method (FEM) in space is used ([2]). Linear conforming elements are chosen in this study. They provide a simple implementation in combination with a guaranteed optimal convergence rate and parallel scalability of the applied AMG preconditioner. To apply the linear FEM discretization to the voxel domain, each voxel is split into six tetrahedra. To solve the bio-heat equation, after the space discretization, the time derivative is discretized via finite differences and the backward Euler scheme is used ([3]).

Let us denote with $K^*$ the stiffness matrix coming from the FEM discretization of the Laplace equation (3). It can be written in the form

$$K^* = \left[ \int_\Omega \sigma \nabla \Phi_i \cdot \nabla \Phi_j d\mathbf{x} \right]_{i,j=1}^{N},$$

where $\{\Phi_i\}_{i=1}^N$ are the FEM basis functions.

The system of linear algebraic equations

$$K^* X = 0 \tag{4}$$

is to be solved to find the nodal values $X$ of the potential distribution.

The electric field intensity and the current density are than expressed by the partial derivatives of the potential distribution in each finite element. This way, the nodal values $F$ for the thermal energy $E \cdot J$ arising from the current flow are obtained.

Let us now turn our attention to the discrete formulation of the bio-heat equation. Let us denote with $K$ and $M$ the stiffness and mass matrices from the finite element discretization of (1). They can be written as

$$K = \left[ \int_\Omega k \nabla \Phi_i \cdot \nabla \Phi_j d\mathbf{x} \right]_{i,j=1}^{N},$$

$$M = \left[ \int_\Omega \rho c \Phi_i \Phi_j d\mathbf{x} \right]_{i,j=1}^{N}.$$

Let us also denote with $\Omega_{bl}$ the subdomain of $\Omega$ occupied by blood vessels and with $M_{bl}$ the matrix

$$M_{bl} = \left[ \int_\Omega \delta_{bl} h_{bl} \Phi_i \Phi_j d\mathbf{x} \right]_{i,j=1}^{N},$$

where

$$\delta_{bl}(x) = \begin{cases} 1 \text{ for } x \in \Omega_{bl}, \\ 0 \text{ for } x \in \Omega \setminus \Omega_{bl}. \end{cases}$$

**TABLE 1.** Thermal and electrical properties of the materials

| **Material** | $\rho$ **(kg/m$^3$)** | $c$ **(J/kg K)** | $k$ **(W/m K)** | $\sigma$ **(S/m)** |
|---|---|---|---|---|
| Ni-Ti | 6 450 | 840 | 18 | $1 \times 10^8$ |
| Stainless steel | 21 500 | 132 | 71 | $4 \times 10^8$ |
| Liver | 1 060 | 3 600 | 0.512 | 0.333 |
| Blood | 1 000 | 4 180 | 0.543 | 0.667 |
| Polyurethane | 70 | 1 045 | 0.026 | $10^{-5}$ |

Than, the parabolic equation (1) can be written in matrix form as:

$$M\frac{\partial T}{\partial t} + (K + M_{bl})T = F + M_{bl}T_{bl}. \tag{5}$$

If we denote with $\tau$ the time-step, with $T^{n+1}$ the solution at the current time level, and with $T^n$ the solution at the previous time level and approximate the time derivative in (5) we obtain the following system of linear algebraic equations for the nodal values of $T^{n+1}$

$$AT^{n+1} = MT^n + \tau G, \tag{6}$$

where

$$A = M + \tau(K + M_{bl}),$$

and

$$G = F + M_{bl}T_{bl}.$$

The matrices $K^*$ and $A$ of the linear systems (4) and (6) are ill-conditioned and very large, having around $10^8$ rows. Since they are symmetric and positive definite, we use the PCG [1] method, which is the most efficient solution method in this case.

A parallel algebraic multigrid implementation is used as a preconditioner. Since the matrix $A$ is not varied between time steps, we only construct the algebraic multigrid once, before the first time-step. It can be readily used after that to precondition the linear systems for all subsequent time steps.

## EXPERIMENTAL RESULTS

The results presented in this section are based on a high-resolution voxel-based representation of the computational domain. The domain consists of liver and tumor tissues, a large bifurcated blood vessel and the RF ablation probe (see Figure 2). Domains with four different sizes ($256 \times 256 \times 256$, $322 \times 322 \times 322$, $406 \times 406 \times 406$, and $512 \times 512 \times 512$), each having approximately twice as many degrees of freedom as the previous, are used to illustrate the weak scalability of the considered solution methods.

Table 1 lists the thermal and electrical properties of the materials, which are taken from [5] as well as the blood perfusion coefficient $w_{bl} = 6.4 \times 10^{-3}$ 1/s.

For the test simulations, a RF voltage of 10 V is applied for a duration of 8 minutes. A time step of $\tau = 5$ s is used. Plots of the output for both the electrical and the thermal

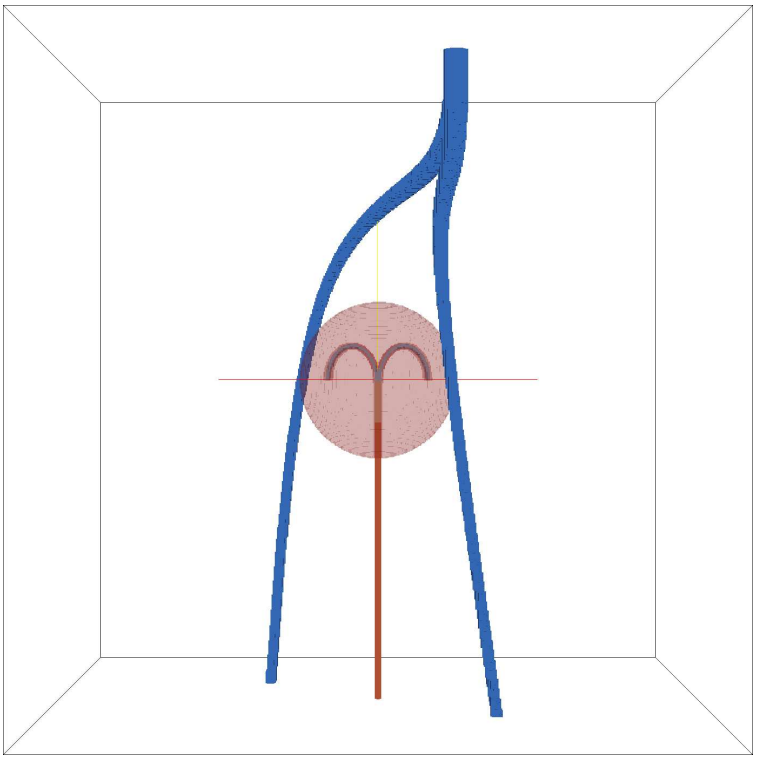

**FIGURE 2.** 3D voxel representation of the computational domain with resolution $512 \times 512 \times 512$

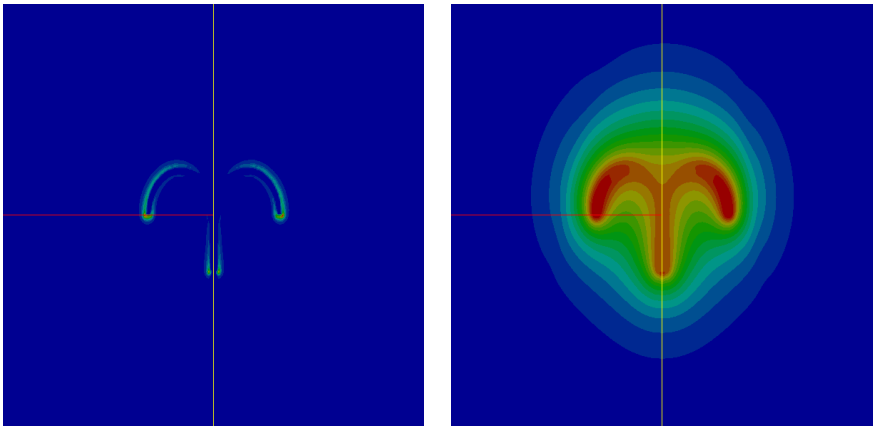

(a) (b)

**FIGURE 3.** Simulation results: (a) energy induced by electricity flow; (b) temperature of the domain after 8 minutes

**TABLE 2.** Parallel times and weak scaling for the complete simulation

| Domain size | Processors | Unknowns | Simulation time | Weak scaling |
|---|---|---|---|---|
| $256 \times 256 \times 256$ | 16 | 16 974 593 | 3 301.07 s | |
| $322 \times 322 \times 322$ | 32 | 33 698 267 | 3 663.99 s | 90 % |
| $406 \times 406 \times 406$ | 64 | 67 419 143 | 4 443.94 s | 74 % |
| $512 \times 512 \times 512$ | 128 | 135 005 697 | 5 235.53 s | 63 % |

parts of the model are presented in Figure 3. Both the maximum value of the heat source and the maximum tissue temperature are located close to the tips of the electrodes.

Large-scale systems of linear algebraic equations arise from the FEM discretization of the considered problem, requiring an efficient parallel implementation. A parallel PCG solver is used here. BoomerAMG [4, 7] is the preconditioner. A relative PCG stopping criterion in the form

$$\mathbf{r}_k^T C^{-1} \mathbf{r}_k \leq \varepsilon^2 \mathbf{r}_0^T C^{-1} \mathbf{r}_0, \qquad \varepsilon = 10^{-6},$$

where $\mathbf{r}_k$ stands for the residual at the $k$-th step of the PCG method, is used.

The settings for the BoomerAMG preconditioner were carefully tuned for maximum scalability in time. The selected coarsening algorithm is *Falgout-CLJP*. *Modified classical interpolation* is applied. The selected relaxation method is *hybrid symmetric Gauss-Seidel or SSOR* in lexicographical ordering on each processor. To decrease the operator and grid complexities two levels of aggressive coarsening are used and the maximum number of elements per row for the interpolation is restricted to six. Smaller operator and grid complexities lead to faster iterations and reduced memory requirements, but can also affect the convergence rate of the solver. Thus, the values of the last two parameters must be carefully chosen to provide the best balance. With the above described setup, the solutions of the linear systems on each time step required 5–6 PCG iterations.

The presented parallel tests are performed on the IBM Blue Gene/P machine at the Bulgarian Supercomputing Center (see http://www.scc.acad.bg/). This supercomputer consists of 2048 PowerPC 450 based compute nodes, each with four cores running at 850 MHz and 2 GB RAM. It is equipped with a torus network for the point to point communications capable of 5.1 GB/s and a tree network for global communications with a bandwidth of 1.7 GB/s. Our code is compiled using the IBM XL C++ compiler with the following options: "`-O5 -qstrict`".

The parallel times for the whole numerical simulation are presented in Table 2. The weak scaling with respect to the smallest simulation domain is also shown.

## CONCLUDING REMARKS

A voxel-based simulation of the RF ablation procedure is presented. This approach can be easily applied to real-life CT scans of a patient's liver. Large-scale linear systems arise from high-resolution CT images. The time-dependent nature of the bio-heat equation requires many such systems to be solved in the course of a single simulation. In this situation, the need of supercomputing resources arises. The presented parallel tests

illustrate the efficiency of the selected parallel solution methods on the Blue Gene/P massively parallel computer.

## ACKNOWLEDGMENTS

This work is partly supported by the Bulgarian NSF Grants DCVP 02/1 (DO02-115/08) and DO02-147/08. We also kindly acknowledge the support of the Bulgarian Supercomputing Center for the access to the IBM Blue Gene/P supercomputer. Last but not least, we would like to thank Theodor Popov (AMET Ltd.) for the constructive discussions and comments on the engineering aspects of tumor ablation.

## REFERENCES

1. O. Axelsson, *Iterative Solution Methods*, Cambridge University Press, 1996.
2. S. Brenner and L. Scott, *The Mathematical Theory of Finite Element Methods. Texts in Applied Mathematics*, **15**, Springer-Verlag, 1994.
3. E. Hairer, S.P. Norsett, and G. Wanner *Solving Ordinary Differential Equations I, II*, Springer Series in Comp. Math., 2000, 2002
4. V.E. Henson and U.M. Yang, BoomerAMG: A parallel algebraic multigrid solver and preconditioner, *Applied Numerical Mathematics* **41**(1), Elsevier, 155–177 (2002).
5. S. Tungjitkusolmun, S.T. Staelin, D. Haemmerich, J.Z. Tsai, H. Cao, J.G. Webster, F.T. Lee, D.M. Mahvi, and V.R. Vorperian, Three-dimensional finite-element analyses for radio-frequency hepatic tumor ablation, *IEEE transactions on biomedical engineering* **49**(1), 3–9 (2002).
6. S. Tungjitkusolmun, E.J. Woo, H. Cao, J.Z. Tsai, V.R. Vorperian, and J.G. Webster, Thermal-electrical finite element modelling for radio frequency cardiac ablation: Effects of changes in myocardial properties, *Medical and Biological Engineering and Computing* **38**(5), 562–568 (2000).
7. Lawrence Livermore National Laboratory, *Scalable Linear Solvers Project*, http://www.llnl.gov/CASC/linear_solvers/.